Bonding performance of Chinese fir heartwood and sapwood with different coatings under a high voltage electric field

Qian He (007589@yzu.edu.cn)
Yangzhou University
QianQian Hou
Yangzhou University
Fangxin Wang
Yangzhou University
Daiyuan Zhang
Nanjing Forestry University
Yong Yang
Tianyi Zhan
Nanjing Forestry University
Dingyi Yang
Yangzhou University
shengcai Li
Yangzhou University

Research Article

Keywords: High voltage electric field, Chinese fir, heartwood, coating, bonding strength

Posted Date: July 12th, 2023

DOI: https://doi.org/10.21203/rs.3.rs-3120553/v1

Additional Declarations: No competing interests reported.

Abstract

Inadequate adhesion performance has been observed in the heartwood with high extract content, leading to poor wood durability. To address this issue, we employed a high voltage electric field (HVEF) treatment that combines activation and polarization functions to enhance the bonding strength between wood and the coating layer. The heartwood and sapwood samples were prepared from Chinese fir lumber. Two types of coatings were applied urea formaldehyde (UF) and polydimethylsiloxane (PDMS). The results revealed a higher absorptivity of UF and PDMS on the sapwood compared to the heartwood, attributed to the larger diameter of tracheids and lower extract content, resulting in lower contact angles on the sapwood. Following the HVEF treatment, a reduction in absorptivity was observed for UF on the heartwood, while a decrease in absorptivity was observed for PDMS on the sapwood. This disparity can be attributed to the differential activation and polarization effects of the HVEF treatment on the two types of coatings. The changes in absorptivity were corroborated by the mass gain rate of UF- and PDMS-coated wood samples, with a strong positive correlation observed between the mass gain rate and absorptivity, yielding a correlation coefficient ≥ 79%. The HVEF treatment significantly enhanced the bonding strength of UF-coated heartwood under N-P(-) condition and PDMS-coated sapwood under N-P(+), resulting in the highest increments of 71% and 75%, respectively. Additionally, notable variations in chemical bonds were detected in the FTIR spectrum of UF-coated heartwood under N-P(-), indicating an increased cross-linking extent between the heartwood and UF chemical groups.

1 Introduction

Engineered wood composites possess significant advantages such as renewability, high specific strength, and carbon fixation capability (Piccardo and Hughes 2022). However, wood is susceptible to degradation, deformation, and cracking due to its natural polymeric components and exposed hydroxyl groups, which enable water absorption or desorption in the environment (Thybring et al. 2018; Zhan et al. 2021). Therefore, enhancing the thermal/light stability and hydrophobicity of wood is crucial for its long-term utilization in engineering and construction. Currently, various functional coatings, such as melamine-urea formaldehyde (MUF) resin, epoxy resins, succinic anhydride, and organic silicon polymers with nanoparticles, are widely applied to wood using immersion, brushing, or grafting methods to protect it from moisture and flame (Cai et al. 2007; Wang et al. 2021a; Wang et al. 2019; Wang et al. 2020; Xu et al. 2020; Zhang et al. 2022).

Nevertheless, fissures and debonding can easily occur when exposed to natural climatic conditions at the interface between the coating and the wood substrate. Consequently, this leads to a deterioration in the bonding property between the coating and the wood, compromising the protective effectiveness of the surface coating and reducing its durability (Feist 1990). Comprehensive investigations conducted by George (2005) have demonstrated that the protective capacity of coatings on wood depends not only on the inherent properties of the coatings but also on the cohesive synergy established at the interface between the wood and the coating. Previous studies have explored various methods to enhance the bonding strength between the wood surface and the coating layer, including increasing the wood surface

roughness, employing silane coupling agents, and conducting plasma treatments. VitosytĖ et al. (2012) reported that increasing the wood surface roughness effectively enhances the mechanical interlocking area between the coating and the wood, thereby improving the bonding strength by 20–34%. Other studies have shown that utilizing methods such as radio frequency oxygen or atmospheric pressure dielectric barrier discharge (DBD) plasma treatment increases the presence of free radicals and polar functional groups on poplar veneer surfaces, modifies the surface morphology, and enhances the surface roughness. Consequently, the bonding strength of plywood improved by 15% and 40%, respectively (Chen et al. 2016; Tang et al. 2015). Denes and Young (1999) employed plasma treatment to enhance the adhesion between PDMS coatings and substrates, and the results indicated that plasma-treated coating samples exhibited lower mass loss and reduced degradation compared to untreated materials after two weeks of weathering, effectively improving the weather resistance of wood. Liu et al. (2020) modified the surface of birch wood using silane coupling agents and investigated the bonding strength between the modified wood surface and the coating. The results demonstrated a significant increase in the bonding strength of samples treated with three different silane coupling agents, with improvements of 354.62%, 316.92%, and 44.62%, respectively (Chen et al. 2017; Duan et al. 2022; Konnerth et al. 2014; Kwon et al. 2014).

However, previous research has indicated that a high content of extracted substances negatively affects the bonding strength between the wood and the coating (Acda et al. 2012). During the transition from sapwood to heartwood, minimal changes occur in the composition of cell walls, but heartwood accumulates more extractives within the cell walls, leading to a darker color (Cao et al. 2020; Li et al. 2019; Song et al. 2014; Yang et al. 2021). A study conducted by Kaygin and Tankut (2008) demonstrated the correlation between adhesive bonding strength and the chemical composition of sapwood and heartwood. Compared to sapwood, excessive extractives in heartwood alter the adhesive's pH value, impeding its curing process and resulting in decreased bonding strength. Nussbaum and Sterley (2002) investigated the influence of wood extractive content on adhesive bonding strength and found that as the extractive content increases, the bonding strength of specimens exposed to boiling water significantly decreases. Additionally, sapwood exhibits greater pore volume and specific surface area compared to heartwood (Cao et al. 2020; Yang et al. 2021). The total pore volumes of sapwood's earlywood and latewood are 0.0046 cm^3/g and 0.0030 cm^3/g, respectively, while in heartwood, they are 0.0039 cm^3/g and 0.0024 cm^3/g, respectively, representing a reduction of 15% and 20%. These pore structures also influence the bonding strength between heartwood, sapwood, and the coating (Kaygin and Tankut 2008; Li et al. 2021; Nussbaum and Sterley 2002; Yin et al. 2015). Furthermore, certain coating agents with chemical inertness, non-polarity, and low surface energy, such as PDMS and modified organic silicon, have a more detrimental effect on the bonding property of heartwood (Jin et al. 2012).

Based on prior research, the activation effect of electric fields enhances the surface activity of materials, intensifies crosslinking reactions, and improves the bonding strength of composites. Studies have demonstrated that electric fields can activate adhesives and adhered components, redistributing charges in the functional groups of the adhesive composition. Simultaneously, the polarization effect of the

electric field regulates diffusion and migration processes, promoting chemical reactions at the bonding interphase. This leads to an increase in bonding strength by 15–90% (Akram Bhuiyan et al. 2020). Galikhanov et al. employed a constant direct current electric field treatment method to prepare UF plywood. Under the polarization effect, the surface free energy of the adhesive increased, and the thickness expansion rate of the board significantly decreased, resulting in elevated bonding strength (Galikhanov et al. 2020; Galikhanov et al. 2018). Similarly, Popov et al. subjected wood-based composite materials to the combined action of direct current electric fields and ultrasound fields. The findings demonstrated a significant decrease in the viscosity and wetting properties of urea-formaldehyde resin on the wood surface under the influence of physical fields, resulting in a remarkable 196% increase in the bonding strength of the composite materials (Popov et al. 2020). Zamilova et al. (2017) conducted research showing that electric fields induce changes in the structure of the adhesive polymer matrix, leading to the formation of new molecular bonds through macromolecular crosslinking, thereby increasing plywood bonding strength by 135%. When subjected to high-voltage electric fields (> 1 kV), electron excitation in the excited state facilitates the aggregation of more active functional groups on the material surface, thereby promoting an increase in surface free energy. Previous studies have revealed that high-voltage electric field treatment significantly enhances the reactivity of the wood surface and adhesive components, resulting in a continuous, uniform, and dense distribution of adhesive at the bonding interface of wood-based composite materials. Consequently, the density and bonding strength of the bonding interface are greatly improved (He et al. 2019a; He et al. 2019b, 2019c; He et al. 2020). Thus, the high-voltage electric field treatment method could be employed to enhance the reactivity and crosslinking degree of coatings, thereby strengthening the bonding strength between the coating and wood. However, there is a limited number of studies focusing on the bonding performance of heartwood materials with high extractive content and different coatings, especially for low surface energy polymers, under HVEF treatment.

In this study, Chinese fir sapwood and heartwood samples with two types of coatings, UF and PDMS, were selected to investigate their bonding strength under HVEF treatment. The diameter distribution of pores and chemical components in the heartwood and sapwood samples were measured. Additionally, the characteristics of UF and PDMS under HVEF treatment were examined. The wetting behavior, including contact angles and absorptivity, of the two coatings on Chinese fir heartwood and sapwood were explored and compared. Furthermore, the mass gain rate and tensile bonding strength of the two coatings with heartwood and sapwood were tested and compared. The chemical reactions of wood with coating chemical bonds were investigated using FTIR measurements.

2 Materials and methods

2.1 Materials

Samples of heartwood and sapwood were selected from Chinese fir (*Cunninghamia lanceolata*) without any visible defects, originating from the same lumber source. The samples were cut to dimensions of 30 mm (radial) × 30 mm (tangential) × 15 mm (longitudinal, thickness) and subjected to a 24-hour drying

process under vacuum conditions at 103°C. Subsequently, the samples were sealed and stored in a room with a temperature of 25°C and a relative humidity of 65% for two weeks, resulting in a moisture content of 10 ± 2%.

To prepare the urea-formaldehyde (UF) adhesive, UF powder (99 wt%, Qingjun Co. Ltd., Hebei, P.R. China) was mixed with distilled water at a ratio of 2:1. The curing agent, ammonium chloride, was added to the UF powder at a mass dosage of 1%. The viscosity of the UF adhesive was measured as 164.53 MPa·s, and the mole ratio was 1.2:1. Polydimethylsiloxane (PDMS, CAS: 63148–62–9, DowCorning, USA) was used along with its curing agent (Octamethylcyclotetrasiloxane, CAS: 556–67–2) in a mass ratio of 10:1. The viscosity of the PDMS was determined as 5500 MPa·s.

2.2 Distribution of pore size and chemical components measurements

The heartwood and sapwood samples were carefully selected and cut into dimensions of 5 mm × 5 mm × 5 mm for scanning electron microscope (SEM) analysis. Subsequently, the micrographs of the wood cross-sections were processed using Image Pro Plus (IPP) software to determine the pore diameter of wood tracheids and the double thickness of the cell wall. The distribution of pore diameter was analyzed using OriginLab 9.0.

For further analysis, the heartwood and sapwood samples were milled, and the resulting powder was subjected to extraction using a toluene/ethanol solvent mixture (2/1 by volume) for 6 h. The extracted powder was then utilized to measure the lignin, cellulose, and hemicellulose contents following the standardized TAPPI method T222 om-02 and NREL/TP-510–42618 ~ c42622.

2.3 Viscosity, pH and zeta potential measurements for test liquids

The UF and PDMS samples, whether uncharged or charged with positive or negative charge (+/-), were placed in a Teflon beaker and subjected to the high voltage electric field (HVEF) treatment using two plate electrodes for a duration of 4 min under a voltage of 60 kV. Two HVEF treatment directions were employed: P-N and N-P (where P plate was connected to the ground, and N plate was connected to the negative high voltage generator). Therefore, a total of six HVEF conditions were studied: P-N, P-N(-), P-N(+), N-P, N-P(-), and N-P(+). Following the HVEF treatment, the viscosity of UF and PDMS was measured using a viscometer (NDJ-5S, Lichen, P.R. China). Their pH and zeta potential values were obtained using a multi-parameter analysis device (DZS-706, INESA, P.R. China). The HVEF treatment method employed in this study was similar to that described in a previous reference (He et al. 2023).

2.4 Wettability measurement and mass gain rate

A droplet of UF or PDMS was carefully dispensed onto the cross-section of sapwood and heartwood using a syringe, with a controlled speed of 0.05 mL/1s. The contact angle of the test liquid, with or without the HVEF treatment, was recorded using a high-speed microscope. Additionally, the absorptivity

of the test liquid on the wood surface was measured according to the wetting model (Wang et al. 2015). This wettability measurement was conducted following a similar approach as described in a previous reference (He et al. 2023).

Twenty specimens, including ten heartwood and ten sapwood samples, with dimensions of 50 mm (width) × 50 mm (length) × 5 mm (height), were submerged together in 500 g of PDMS mixed with the curing agent (10/1, by volume) in one beaker. Another set of twenty specimens was submerged in 500 g of UF resin in a separate beaker. Subsequently, both beakers were subjected to the HVEF treatment with a voltage of 60 kV for a duration of 1 h at 23°C. After the HVEF treatment, the soaked specimens were removed from the beakers. The PDMS-coated specimens were then cured at 23°C for 24 h, while the UF-coated specimens were cured at 120°C for 30 min. The mass gain rate (%) was calculated using the following formula:

$$rate(\%) = \frac{(m_{cured} - m_0)}{m_0} \times 100\% \quad (1)$$

where the m_{cured} is the mass of cured specimens, the m_0 is the mass of wood sample without any treatment.

2.5 Tensile bonding strength

The two cross sections of the specimens coated with PDMS or UF layer were bonded to the surface of the tensile fixture using hot melt adhesive (Fig. 1). The tensile bonding strength between PDMS (or UF) and wood was measured using a universal mechanical testing machine (WDW-100, Changchun Machinery Co., Ltd., China) at a loading speed of 1 mm/min.

2.6 Fourier transform infrared spectroscopy (FTIR) measurement

In this study, a Fourier transform infrared spectroscopy device equipped with attenuated total reflection (ATR-FTIR, PerkinElmer Co. Ltd.) was used to record the spectra of the pristine wood, UF, PDMS, UF-coated wood, and PDMS-coated wood samples. The scanning range for the spectra was from 400 to 4000 cm^{-1}.

3 Results and discussion

3.1 Main characteristics of sapwood, heartwood and coating

The wetting behavior of the coating on the wood substrate is significantly influenced by the chemical components and anatomical characteristics of the wood. Chinese fir, for instance, exhibits distinct chemical components and microstructure differences between its heartwood and sapwood, which are

prominent macro-characteristics of wood (Okuno et al. 2009). These chemical and anatomical properties have a substantial impact on the coating's chemical reaction and wettability. As indicated in Table 1, heartwood and sapwood display similar contents of cellulose, hemicellulose, and lignin, while heartwood exhibits a higher extract content of 5.42%. Previous related references have also reported varying extract contents depending on the extraction method. The presence of extracts is attributed to the formation of phenolic compounds during tree growth, which are deposited in the cell wall matrix and pore structure, giving Chinese fir heartwood its darker color (Cao et al. 2020; Yang et al. 2021).

Table 1
Chemical components for Chinese fir heartwood and sapwood

	Cellulose	Lignin	Hemi-cellulose	Extract	Reference
Heartwood	51.98%	32.65%	23.39%	4.14–5.26% (benzene–ethanol)	[34]
	45.5%	32.4%	25.7%	0.51% (Lipophilic)	[35]
	40.15%	33.96%	20.32%	/	[36]
	43.22%	33.42%	24.53%	5.42%	for this study
Sapwood	48.62%	33%	23.1%	1.42–1.71% (benzene–ethanol)	[34]
	47.1%	30.9%	24.3%	0.88% (Lipophilic)	[35]
	43.43%	34.16%	19.86%	/	[36]
	44.56%	32.44%	23.45%	2.16%	for this study

Furthermore, a comparison of pore sizes was conducted between the cross-sections of Chinese fir heartwood and sapwood. As shown in Fig. 2, sapwood has larger pore sizes in the tracheid structure compared to heartwood, as observed from the micrographs and the measured pore diameter distribution. While the majority of pore diameters range from 0 to 10 μm, tracheids with diameters greater than 20 μm still play a significant role in liquid penetration into wood (Singh et al. 2015). In the case of heartwood (Fig. 2a and 2b), the pore diameter is mainly distributed below 65 μm. Additionally, in the latewood region of heartwood, a higher number of tracheids with diameters ranging from 20 to 45 μm are observed, while a lower number falls within the range of 45 to 65 μm compared to the earlywood. In the sapwood (Fig. 2c and 2d), larger tracheid diameters ranging from 70 to 100 μm are found in the earlywood region, while diameters below 70 μm are observed in the latewood. Reference sources report that tracheid diameters in Chinese fir typically range from 20 to 70 μm, varying based on tree growth (Duan et al. 2016).

Furthermore, the cell wall thickness of Chinese fir measures between 5 and 8 μm, with thicker walls observed in the latewood of the heartwood region (Wang et al. 2021b).

In contrast, the HVEF treatment can affect the characteristics of the coating, and thus the viscosity, zeta potential, and pH of UF and PDMS were measured under different electric field conditions. Figure 3 illustrates that PDMS exhibits higher viscosity and zeta potential values compared to UF in the control condition. After the HVEF treatment, PDMS displays increased viscosity under the N-P condition, while UF shows higher viscosity when subjected to the opposite direction of the HVEF. Regarding zeta potential, UF resin exhibits a negative value with a significant decrease, particularly under the N-P(+) condition. Conversely, PDMS shows an increased positive zeta potential under various HVEF conditions. Additionally, UF samples do not exhibit significant changes in pH, whereas PDMS samples experience significant decreases under different conditions except for the P-N(+) condition. These results can be attributed to the activation of charges, functional groups, and electric dipole moments under the electric field, leading to chemical bond recombination and changes in molecular alignment (Andrade and Dodd 1939; Okuno et al. 2009). The contrasting behavior between UF and PDMS arises from differences in the activation and polarization extents of their chemical groups and variations in molecular structure during the HVEF treatment (Deng et al. 2014; Zhu et al. 2013).

3.2 Wettability of different coatings on Chinese fir under the HVEF treatment

The wetting behavior of HVEF-treated UF and PDMS coatings on Chinese fir can be significantly influenced by their varied viscosity, zeta potential, and pH values. Droplets of UF or PDMS were applied to the cross-sections of Chinese fir sapwood and heartwood under the HVEF treatment. The contact angle of UF and PDMS was recorded at different wetting durations, and fitting curves were established to depict the wetting process over a duration of 200 s. Using the wetting model, the decrease rate (K_θ) was calculated based on the fitting curve of contact angle with wetting duration (Fig. 4 and Fig. 5). The absorptivity of the coatings on the heartwood and sapwood was determined from the fitting curve of contact angle with wetting duration, and the increase rates (K_a) were obtained from the fitting curve of absorptivity with wetting duration (Fig. 6 and Fig. 7).

Figures 4 to 7 demonstrate that, in the control condition, UF and PDMS coatings exhibited lower initial contact angle ($CA_{initial}$) and equilibrium contact angle ($CA_{equilibrium}$, CAs) and higher absorptivity on sapwood compared to heartwood, with higher K_θ values. This result can be attributed to the larger tracheid diameter and lower extract content in sapwood compared to heartwood. After the HVEF treatment, Fig. 4a shows that for heartwood, UF coatings exhibited lower CAs under the P-N, P-N(-), P-N(+), and N-P conditions, with increased K_θ values for P-N and P-N(-), while higher CAs were observed under N-P(-) and N-P(+). Similarly, the wetting behavior of UF on sapwood varied under the HVEF treatment. Compared to the control, lower CAs were observed for various conditions, with decreased K_θ values except for P-N(+) and N-P(-) (Fig. 4b).

Regarding the low surface energy and nonpolar nature of PDMS coatings, as shown in Fig. 5 and Fig. 7, higher CAs with higher K_θ values and lower absorptivity of PDMS on Chinese fir were observed in the control condition compared to UF samples. This can be attributed to the higher viscosity of PDMS, as shown in Fig. 3. Additionally, lower $CA_{equilibrium}$ of PDMS was observed on sapwood compared to heartwood, which aligns with the variations observed in UF CAs. After the HVEF treatment, no significant changes in CA_s on heartwood were observed for different conditions, except for N-P(-), which showed a significant change in K_θ (Fig. 5a). Moreover, for sapwood, a decrease in $CA_{initial}$ was observed, but no significant variation in $CA_{equilibrium}$ was found for each condition (Fig. 5b). Consistent with previous studies, it is noted that the electric field does not greatly influence the wetting behavior of nonpolar coatings unless specific voltage conditions of HVEF treatment are selected (Vancauwenberghe et al. 2013).

Moreover, as depicted in Fig. 6, the absorptivity of UF and PDMS coatings on heartwood and sapwood was calculated and compared. In the control condition, UF exhibited higher absorptivity of 82% on sapwood with higher K_θ values compared to heartwood, which was attributed to the lower CAs of UF on sapwood. Compared to the control, decreased absorptivity of UF on heartwood was observed under the P-N(+), N-P, N-P(-), and N-P(+) conditions, with decreased K_a values (Fig. 6a). This result can be attributed to the higher CAs or lower K_θ values obtained after the HVEF treatment, as shown in Fig. 4(a). As for sapwood (Fig. 6b), higher absorptivity of UF was found, especially under the P-N and P-N(+) conditions, which can be attributed to the lower $CA_{equilibrium}$ observed in Fig. 4(b).

Furthermore, for PDMS (Fig. 7), higher absorptivity of 76% was observed on sapwood compared to heartwood. These results were due to the higher $CA_{equilibrium}$ of PDMS on heartwood. Under the HVEF treatment, no significant changes in absorptivity were observed for PDMS on Chinese fir under various HVEF treatments, except for N-P(+) on heartwood and N-P(+) and N-P(-) on sapwood. This can be attributed to the absence of significant variations in $CA_{equilibrium}$ observed under the aforementioned conditions, as shown in Fig. 5. Notably, an increase in absorptivity of PDMS on heartwood was observed under N-P(+), while decreases on sapwood were observed under N-P(+) and N-P(-). This could be attributed to the elongation of PDMS droplets and their shape retention during the HVEF treatment, with no significant changes in CAs but changes in permeability into the wood (Miksis 1981).

This study also revealed distinct differences in wettability between UF and PDMS on Chinese fir, which can be attributed to the different activation and polarization extents during the HVEF treatment, as demonstrated in Fig. 3. However, no significant relationships were observed between the wetting behavior and physical characteristics of the coatings shown in Fig. 3. This could be due to the unstable performance of liquid coatings after the HVEF treatment, which exhibits higher extents of activation and polarization.

3.3 Mass gain rate and tensile bonding strength

To validate the results of absorptivity, further investigation of the mass gain rate was conducted on wood samples immersed in the coatings. As depicted in Fig. 8, the control condition showed higher mass gain rates for sapwood samples compared to heartwood, attributed to the better wettability of sapwood with a larger pore diameter distribution. For the HVEF-treated wood samples, lower mass gain rates of approximately 22% were observed for heartwood. Notably, higher mass gain rates of 44% and 43% were observed for sapwood samples, particularly under the P-N and P-N(+) conditions (Fig. 8a). Positive relationships between mass gain rate and absorptivity were also established, with the correlation coefficent (R^2) values of 86% and 81% for heartwood and sapwood, respectively (Fig. 8c). Similar trends were observed for PDMS, with R^2 values of 79% and 86% for heartwood and sapwood, respectively (Fig. 8d). The highest increase in PDMS mass gain rate for heartwood was observed under the N-P(+) condition, while decreases were observed for sapwood under N-P(-) and N-P(+) (Fig. 8b). These results indicate a strong agreement between the mass gain rate of UF and the variations in absorptivity.

The bonding strength between the coating layer and the wood cross-section surface was also measured for heartwood and sapwood samples. As shown in Fig. 9, UF-coated wood samples exhibited higher bonding strength compared to PDMS-coated wood samples, attributed to the formation of more polar chemical bonds and higher cross-linking extent. After the HVEF treatment, both UF- and PDMS-coated wood samples showed increased bonding strength. Particularly, the highest increment of 71% was observed for UF-coated heartwood samples under the N-P(-) condition. This enhancement in bonding strength aligns with previous studies, attributed to the activation and triggering of chemical groups under the HVEF treatment, providing more reaction sites for UF crosslinking with wood and resulting in lower absorptivity of UF at the bonding interphase (He et al. 2019a). In the case of sapwood, the increment ranged from 7–34% under the HVEF treatment (Fig. 9a). This can be attributed to the larger pore diameter observed in sapwood, which negatively affects the crosslinking reaction between UF and wood under the HVEF treatment, as demonstrated in previous studies (He et al. 2019c). Furthermore, the correlation between absorptivity and bonding strength was established. As expected, a significant R^2 value of 81% was obtained for heartwood, indicating a strong relationship between bonding strength and absorptivity (Fig. 9c). However, no noticeable relationship was observed for sapwood samples. In the case of PDMS-coated wood samples (Fig. 9b), the highest increment of 75% was found for PDMS-coated sapwood samples under the N-P(+) conditions, while no significant variation was observed for the heartwood samples. This result can be attributed to the lower absorptivity of PDMS on sapwood and the higher cross-linking extent between PDMS and sapwood. Moreover, a negative relationship with an R^2 value of 90% was observed between bonding strength and absorptivity for sapwood (Fig. 9d), indicating that higher absorptivity resulted in lower bonding strength.

Furthermore, FTIR spectroscopy was employed to investigate the chemical bonds formed between UF or PDMS and wood functional groups under the HVEF treatment. The chemical structures of untreated wood, UF-coated wood, and PDMS-coated wood were compared (Fig. 10). For untreated UF resin, the peak at 3297 cm^{-1} was assigned to N-H stretching of primary aliphatic amines. Another strong absorption band at 1633 cm^{-1} was attributed to the C = O stretching vibration involved in amide I and II.

The overlapped bands at 1508–1548 cm^{-1} were attributed to C–H stretching vibrations. The small peak at 1439 cm^{-1} may be attributed to C–H bending vibrations of $–CH_2$ and $–CH_3$ groups. The weak absorption band around 1381 cm^{-1} may be ascribed to C–H stretching in CH_2OH. The absorption band at 1013 cm^{-1} was assigned to N–CH_2-N asymmetric stretching vibrations (Samaržija-Jovanović et al. 2016). In untreated wood, the absorption band at 3341 cm^{-1} originated from O–H stretching vibrations. The peak at 2893 cm^{-1} was attributed to –CH stretching vibrations. The bonds at 1731 cm^{-1} and 1656 cm^{-1} were assigned to C = O stretching and –OH bending vibrations. The smaller bonds in the region of 1017 cm^{-1} were attributed to C–O stretching vibrations, and the band at 1596 cm^{-1} was assigned to the C = O stretching vibration of aromatic compounds resulting from accumulated extractives in the cell walls. The band at 1261 cm^{-1} was attributed to C–O–C stretching vibration, and the band at 1424 cm^{-1} was ascribed to C-C benzene ring skeleton vibration and C–H stretching vibration (Samaržija-Jovanović et al. 2016; Xiao et al. 2023).

Compared to the pristine wood, an increased absorption bond at 1633 cm^{-1} attributed to C = O involvement in UF was observed, while decreased bonds at 1731, 3341, 2893, and 1017 cm^{-1} were found for UF-coated heartwood, corresponding to wood chemical groups. These results indicate that a chemical reaction occurred and bonds formed between UF and wood chemical components. Significant variations in the above bonds were observed after HVEF treatment in the spectrum of UF-coated heartwood, suggesting a higher cross-linking extent between wood and UF chemical groups. Additionally, there was a noticeable increase in the intensity of UF absorption bonds, which correlated with the decreased absorptivity of UF on the wood substrate (Fig. 10a). In the spectrum of sapwood sample, lower intensity at the band of 1596 cm^{-1} and higher intensity at the bands of 3341, 2893, and 1013 cm^{-1} were found compared to heartwood, indicating lower extractive content in sapwood (Song et al. 2014) (Fig. 10b). While a similar chemical structure was observed for UF-coated sapwood compared to UF-coated heartwood, lower band intensity was observed after HVEF treatment. This could explain the higher increment in bonding strength for UF-coated heartwood (71%) compared to sapwood (34%).

Moreover, the infrared spectrum of PDMS is shown in Fig. 10c and 10d. The asymmetric contraction peak of the C–H band appeared at 2966 cm^{-1}. The absorption bands at 1411 cm^{-1} and 1257 cm^{-1} were assigned to the Si–CH_3 group. The typical bands at 866 cm^{-1} and 785 cm^{-1} corresponded to symmetrical stretching vibrations. The band at 1005 cm^{-1} represented the asymmetric stretching vibration of the Si-O-Si framework (Xiao et al. 2023). In the spectrum of PDMS-coated wood, the bands at 2966, 1411, 1257, and 1005 cm^{-1} associated with PDMS covered the bands of 2893, 1424, 1261, and 1017 cm^{-1} attributed to wood components, indicating the formation of effective combination bonds between PDMS and wood functional groups. After HVEF treatment, higher intensity of the aforementioned chemical bands was observed in PDMS-coated sapwood samples, while no significant variation in the bands was observed for PDMS-coated heartwood. This suggests a greater occurrence of cross-linked reactions between PDMS and sapwood chemical groups, which aligns with the decreased absorptivity of PDMS on the sapwood surface. The decreased absorptivity of UF and PDMS, along with

their higher cross-linking extent with wood, contributes to the enhancement mechanism of bonding strength under HVEF treatment.

4 Conclusions

The application of HVEF treatment has a positive impact on the bonding strength between the heartwood and the UF coating layer under the N-P(-) condition. This can be attributed to the decreased absorptivity of the coating on the heartwood and a higher degree of cross-linking between their chemical bonds. Furthermore, a significant correlation between the absorptivity of UF on heartwood and its bonding strength was observed with an R^2 value of 81%. However, the HVEF treatment did not have a significant effect on the bonding strength of PDMS-coated heartwood samples.

Regarding the wettability of coatings on Chinese fir, the higher absorptivity of both UF and PDMS was found on sapwood compared to heartwood. This can be attributed to the larger diameter of tracheids and lower extract content, resulting in lower CAs on the sapwood surface. After the HVEF treatment, the absorptivity of UF decreased on the heartwood, while the absorptivity of PDMS decreased on the sapwood. The differing results in wettability between UF and PDMS can be attributed to the different degrees of activation and polarization during the HVEF treatment. This study contributes to the understanding of improving wood bonding strength with different coatings and enhancing wood durability.

Declarations

Ethical Approval Our research did not involve human or animal studies.

Competing interests The authors declare there is no conflict of interest.

Authors' contributions Qian He: Writing- Reviewing and Editing;QianQian Hou: Data curation, Writing-Original draft preparation;Fangxin Wang:Conceptualization, Methodology, Software; Daiyuan Zhang: Visualization, Investigation;Tianyi Zhan:Software,Validation;Dingyi Yang:Reviewing;Yong Yang:Supervision;Shengcai Li:Supervision.All authors read and approved the final manuscript.

Acknowledgements: The authors appreciated the foundations from the Postgraduate Research & Practice Innovation Program of Jiangsu Province (SJCX22_1754), the Natural Science Foundation of the Jiangsu Higher Education Institutions of China (22KJB560032), Jiangsu Province Postdoctoral Science Foundation (2021K474C) and the International cooperation research program of Yangzhou (YZ2019148).

Availability of data and materials All data generated and analyzed during this study are available from the corresponding authors on reasonable request.

References

1. Acda MN, Devera EE, Cabangon RJ, Ramos HJ (2012) Effects of plasma modification on adhesion properties of wood. Int J Adhes Adhes 32: 70-75. https://doi.org/10.1016/j.ijadhadh.2011.10.003
2. Akram Bhuiyan MS, Roland JD, Liu B, Reaume M, Zhang Z, Kelley JD, Lee BP (2020) In situ deactivation of catechol-containing adhesive using electrochemistry. J Am Chem Soc 142: 4631-4638. https://doi.org/10.1021/jacs.9b11266
3. Andrade ENdC, Dodd C (1939) Effect of an electric field on the viscosity of liquids. Nature 144: 117-118. https://doi.org/10.1038/144117b0
4. Cai X, Riedl B, Zhang SY, Wan H (2007) Effects of nanofillers on water resistance and dimensional stability of solid wood modified by melamine-urea-formaldehyde resin. Wood Fiber Sci: 307-318. https://wfs.swst.org/index.php/wfs/article/view/1837/1837
5. Cao S, Zhang Z, Sun Y, Li Y, Zheng H (2020) Profiling of widely targeted metabolomics for the identification of secondary metabolites in heartwood and sapwood of the Red-Heart Chinese Fir (Cunninghamia Lanceolata). Forests 11: 897. https://doi.org/10.3390/f11080897
6. Chen L, Wang Y, Fei P, Jin W, Xiong H, Wang Z (2017) Enhancing the performance of starch-based wood adhesive by silane coupling agent (KH570). Int J Biol Macromol 104: 137-144. https://doi.org/10.1016/j.ijbiomac.2017.05.182
7. Chen M, Zhang R, Tang L, Zhou X, Li Y, Yang X (2016) Effect of plasma processing rate on poplar veneer surface and its application in plywood. BioResources 11: 1571-1584. https://doi.org/10.15376/biores.11.1.1571-1584
8. Denes AR, Young RA (1999) Reduction of weathering degradation of wood through plasma-polymer coating. Holzforschung 53: 632-640. https://doi.org/10.1515/HF.1999.104
9. Deng S, Pizzi A, Du G, Zhang J, Zhang J (2014) Synthesis, structure, and characterization of glyoxal-urea-formaldehyde cocondensed resins. J Appl Polym Sci 131: 41009. https://doi.org/10.1002/app.41009
10. Duan H, Cao S, Zheng H et al. (2016) Variation in the growth traits and wood properties of Chinese fir from six provinces of southern China. Forests 7: 192. https://doi.org/10.3390/f7090192
11. Duan Z, Hu M, Jiang S, Du G, Zhou X, Li T (2022) Cocuring of epoxidized soybean oil-based wood adhesives and the enhanced bonding performance by plasma treatment of wood surfaces. ACS Sustain Chem Eng 10: 3363-3372. https://doi.org/10.1021/acssuschemeng.2c00130
12. Feist WC (1990) Outdoor wood weathering and protection. Archaeol Wood Propert Chem Preserv 225: 263-298. https://doi.org/10.1021/ba-1990-0225.ch011
13. Galikhanov MF, Domracheva AF, Yovcheva T, Exner G (2020) On the origin of changes in the adhesive interaction between veneer and glue under glue polarization in plywood manufacture. Polym Sci Ser D 13: 123-128. https://doi.org/10.1134/S1995421220020069
14. Galikhanov MF, Platonova PA, Zamilova AF (2018) Influence of Polarization of Urea-Formaldehyde Glue in the Process of Manufacture of Plywood on Its Water and Moisture Absorption. Polym Sci Ser D 11: 122-126. https://doi.org/10.1134/S1995421218020065

15. George B, Suttie E, Merlin A, Deglise X (2005) Photodegradation and photostabilisation of wood–the state of the art. Polym Degr Stab 88: 268-274. https://doi.org/10.1016/j.polymdegradstab.2004.10.018
16. He Q, Hou Q, Wang F et al. (2023) High-voltage electric field-induced decreased absorption efficiency of phenol formaldehyde adhesive in different sections of Chinese fir wood. Eur J Wood Wood Prod 81: 493-505. https://doi.org/10.1007/s00107-022-01892-6
17. He Q, Zhan T, Ju Z, Zhang H, Hong L, Brosse N, Lu X (2019a) Influence of high voltage electrostatic field (HVEF) on bonding characteristics of Masson (Pinus massoniana Lamb.) veneer composites. Eur J Wood Wood Prod 77: 105-114. https://doi.org/10.1007/s00107-018-1360-6
18. He Q, Zhan T, Zhang H, Ju Z, Hong L, Brosse N, Lu X (2019b) Robust and durable bonding performance of bamboo induced by high voltage electrostatic field treatment. Ind Crops Prod 137: 149-156. https://doi.org/10.1016/j.indcrop.2019.05.010
19. He Q, Zhan T, Zhang H, Ju Z, Hong L, Brosse N, Lu X (2019c) Variation of surface and bonding properties among four wood species induced by a high voltage electrostatic field (HVEF). Holzforschung 73: 957-965. https://doi.org/10.1515/hf-2018-0190
20. He Q, Zhan T, Zhang H, Ju Z, Hong L, Xiaoning L (2020) Prediction of stiffness and strength distributions in laminated-wood treated by high voltage electrostatic field (HVEF). Mater Today Commun 24: 101186. https://doi.org/10.1016/j.mtcomm.2020.101186
21. Jin X, Strueben J, Heepe L et al. (2012) Joining the un-joinable: adhesion between low surface energy polymers using tetrapodal ZnO linkers. Adv Mater 24: 5676-5680. https://doi.org/10.1002/adma.201201780
22. Kaygin B, Tankut AN (2008) Comparison of bonding strengths of the sapwoods and heartwoods of tree species used in wooden shipboard building. African J Biotechnol 7: 4620-4627. https://www.ajol.info/index.php/ajb/article/view/59648/47936
23. Konnerth J, Weigl M, Gindl-Altmutter W et al. (2014) Effect of plasma treatment on cell-wall adhesion of urea-formaldehyde resin revealed by nanoindentation. Holzforschung 68: 707-712. https://doi.org/10.1515/hf-2013-0130
24. Kwon OM, See SJ, Kim SS, Hwang HY (2014) Effects of surface treatment with coupling agents of PVDF-HFP fibers on the improvement of the adhesion characteristics on PDMS. Applied Surf Sci 321: 378-386. https://doi.org/10.1016/j.apsusc.2014.10.028
25. Li Y, Deng X, Zhang Y et al. (2019) Chemical characteristics of heartwood and sapwood of red-heart Chinese fir (Cunninghamia lanceolata). Forest Prod J 69: 103-109. https://doi.org/10.13073/FPJ-D-18-00042
26. Li Y, Li C, Song Y, Guo Y, Yao L (2021) Anatomical, physical, and mechanical parameters of clone plantation tree, cunninghamia lanceolata. BioResources 16: 3494-3519. https://doi.org/10.15376/biores.16.2.3494-3519
27. Liu W, Hu C, Zhang W, Liu Z, Shu J, Gu J (2020) Modification of birch wood surface with silane coupling agents for adhesion improvement of UV-curable ink. Progr Org Coat 148: 105833.

https://doi.org/10.1016/j.porgcoat.2020.105833

28. Miksis MJ (1981) Shape of a drop in an electric field. Phys Fluids 24: 1967-1972. https://doi.org/10.1063/1.863293
29. Nussbaum RM, Sterley M (2002) The effect of wood extractive content on glue adhesion and surface wettability of wood. Wood Fiber Sci: 57-71. https://wfs.swst.org/index.php/wfs/article/view/612/612
30. Okuno Y, Minagawa M, Matsumoto H, Tanioka A (2009) Simulation study on the influence of an electric field on water evaporation. J Mol Struct THEOCHEM 904: 83-90. https://doi.org/10.1016/j.theochem.2009.02.035
31. Piccardo C, Hughes M (2022) Design strategies to increase the reuse of wood materials in buildings: Lessons from architectural practice. J Clean Prod 368: 133083. https://doi.org/10.1016/j.jclepro.2022.133083
32. Popov V, Latynin A, Tinkov A (2020) Combined physical modification of polymer adhesives used in woodworking.*IOP Conference Series: Earth and Environmental Science*. International Forestry Forum "Forest Ecosystems as Global Resource of the Biosphere: Calls, Threats, Solutions", 23 October. IOP Publishing, Voronezh, Russian Federation, pp 012061. https://doi.org/10.1088/1755-1315/595/1/012061
33. Samaržija-Jovanović S, Jovanović V, Petković B, Dekić V, Marković G, Zeković I, Marinović-Cincović M (2016) Nanosilica and wood flour-modified urea–formaldehyde composites. J Thermopl Compos Mater 29: 656-669. https://doi.org/10.1177/0892705714531977
34. Singh AP, Nuryawan A, Park B-D, Lee KH (2015) Urea-formaldehyde resin penetration into Pinus radiata tracheid walls assessed by TEM-EDXS. Holzforschung 69: 303-306. https://doi.org/10.1515/hf-2014-0103
35. Song K, Yin Y, Salmén L, Xiao F, Jiang X (2014) Changes in the properties of wood cell walls during the transformation from sapwood to heartwood. J Mater Sci 49: 1734-1742. https://doi.org/10.1007/s10853-013-7860-1
36. Tang L, Zhang R, Wang X, Yang X, Zhou X (2015) Surface modification of poplar veneer by means of radio frequency oxygen plasma (RF-OP) to improve interfacial adhesion with urea-formaldehyde resin. Holzforschung 69: 193-198. https://doi.org/10.1515/hf-2014-0018
37. Thybring EE, Kymäläinen M, Rautkari L (2018) Experimental techniques for characterising water in wood covering the range from dry to fully water-saturated. Wood Sci Technol 52: 297-329. https://doi.org/10.1007/s00226-017-0977-7
38. Vancauwenberghe V, Di Marco P, Brutin D (2013) Wetting and evaporation of a sessile drop under an external electrical field: A review. Coll Surf A Physicochem Eng Asp 432: 50-56. https://doi.org/10.1016/j.colsurfa.2013.04.067
39. VitosytĖ J, UkvalbergienĖ K, Keturakis G (2012) The effects of surface roughness on adhesion strength of coated ash (Fraxinus excelsior L.) and birch (Betula L.) wood. Mater Sci 18: 347-351. https://doi.org/10.5755/j01.ms.18.4.3094

40. Wang D, Ling Q, Nie Y, Zhang Y, Zhang W, Wang H, Sun F (2021a) In-situ cross-linking of waterborne epoxy resin inside wood for enhancing its dimensional stability, thermal stability, and decay resistance. ACS Appl Polym Mater 3: 6265-6273. https://doi.org/10.1021/acsapm.1c01070
41. Wang W, Zhu Y, Cao J, Sun W (2015) Correlation between dynamic wetting behavior and chemical components of thermally modified wood. Appl Surf Sci 324: 332-338. https://doi.org/10.1016/j.apsusc.2014.10.139
42. Wang Y, Jia R, Sun H, Liu Y, Lyu J, Zhao R, Liu S (2021b) Wood mechanical properties and their correlation with microstructure in Chinese fir clones. IAWA J 42: 497-506. https://doi.org/10.1163/22941932-bja10047
43. Wang Y, Yan W, Frey M, Vidiella del Blanco M, Schubert M, Adobes-Vidal M, Cabane E (2019) Liquid-like SiO2-g-PDMS coatings on wood surfaces with underwater durability, antifouling, antismudge, and self-healing properties. Adv Sustain Syst 3: 1800070. https://doi.org/10.1002/adsu.201800070
44. Wang Z, Han X, Wang S, Lv Y, Pu J (2020) Enhancing the thermal stability, water repellency, and flame retardancy of wood treated with succinic anhydride and melamine-urea-formaldehyde resins. Holzforschung 74: 957-965. https://doi.org/10.1515/hf-2019-0213
45. Xiao Z, Wang Y, Song Y, Li Q, Xu Q, Li J (2023) Functional improvement of fast-growing wood based on nano-ZnO/PDMS double-layer structure. Wood Sci Technol 57: 275-288. https://doi.org/10.1007/s00226-022-01441-7
46. Xu E, Zhang Y, Lin L (2020) Improvement of mechanical, hydrophobicity and thermal properties of Chinese fir wood by impregnation of nano silica sol. Polymers 12: 1632. https://doi.org/10.3390/polym12081632
47. Yang X, Yu X, Liu Y et al. (2021) Comparative metabolomics analysis reveals the color variation between heartwood and sapwood of Chinese fir (Cunninghamia lanceolata (Lamb.) Hook. Ind Crops Prod 169: 113656. https://doi.org/10.1016/j.indcrop.2021.113656
48. Yin J, Song K, Lu Y, Zhao G, Yin Y (2015) Comparison of changes in micropores and mesopores in the wood cell walls of sapwood and heartwood. Wood Sci Technol 49: 987-1001. https://doi.org/10.1007/s00226-015-0741-9
49. Zamilova A, Galikhanov M, Safin R, Ziatdinov R, Mikryukova Y (2017) Change of the properties of plywood during the thermomodification of veneer and the polarization of the glue. IV International Young Researchers' Conference: Physics, Technologies and Innovation, 15-19 May. AIP Publishing LLC, Russia, pp 020053. https://doi.org/10.1063/1.5002950
50. Zhan T, Lyu J, Eder M (2021) In situ observation of shrinking and swelling of normal and compression Chinese fir wood at the tissue, cell and cell wall level. Wood Sci Technol 55: 1359-1377. https://doi.org/10.1007/s00226-021-01321-6
51. Zhang X, Song S, Li X et al. (2022) Effect of low molecular weight melamine-urea-formaldehyde resin impregnation on poplar wood pore size distribution and water sorption. Ind Crops Prod 188: 115700. https://doi.org/10.1016/j.indcrop.2022.115700

52. Zhu L, Xue J, Wang Y, Chen Q, Ding J, Wang Q (2013) Ice-phobic coatings based on silicon-oil-infused polydimethylsiloxane. ACS Appl Mater Interf 5: 4053-4062. https://doi.org/10.1021/am400704z

Figures

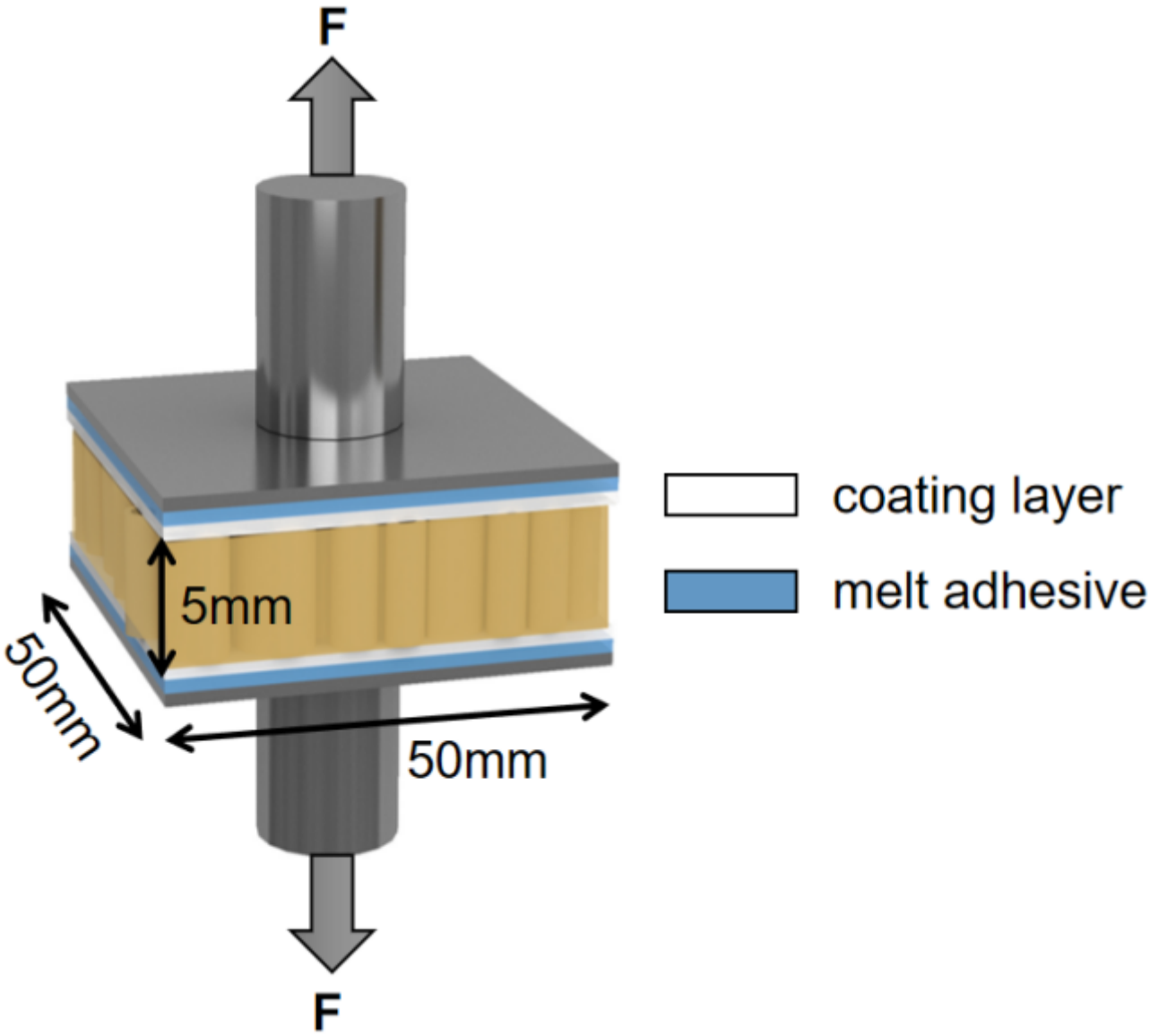

Figure 1

The diagram for the tensile bonding strength of coating layer with wood cross section surface.

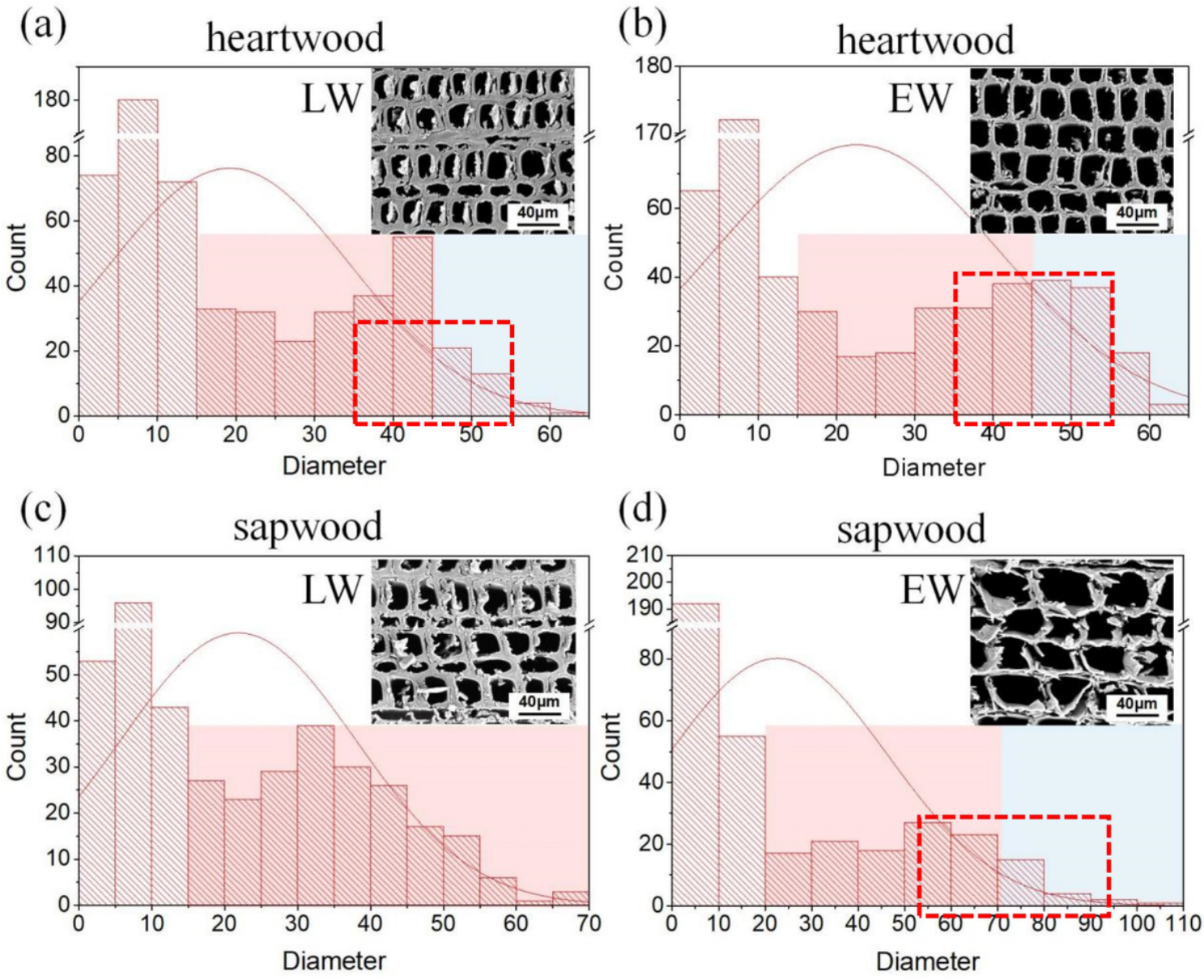

Figure 2

The pore diameter distribution of Chinese fir (a) heartwood latewood, (b) earlywood, (c) sapwood latewood and (d) earlywood, respectively. LW: latewood, EW: earlywood.

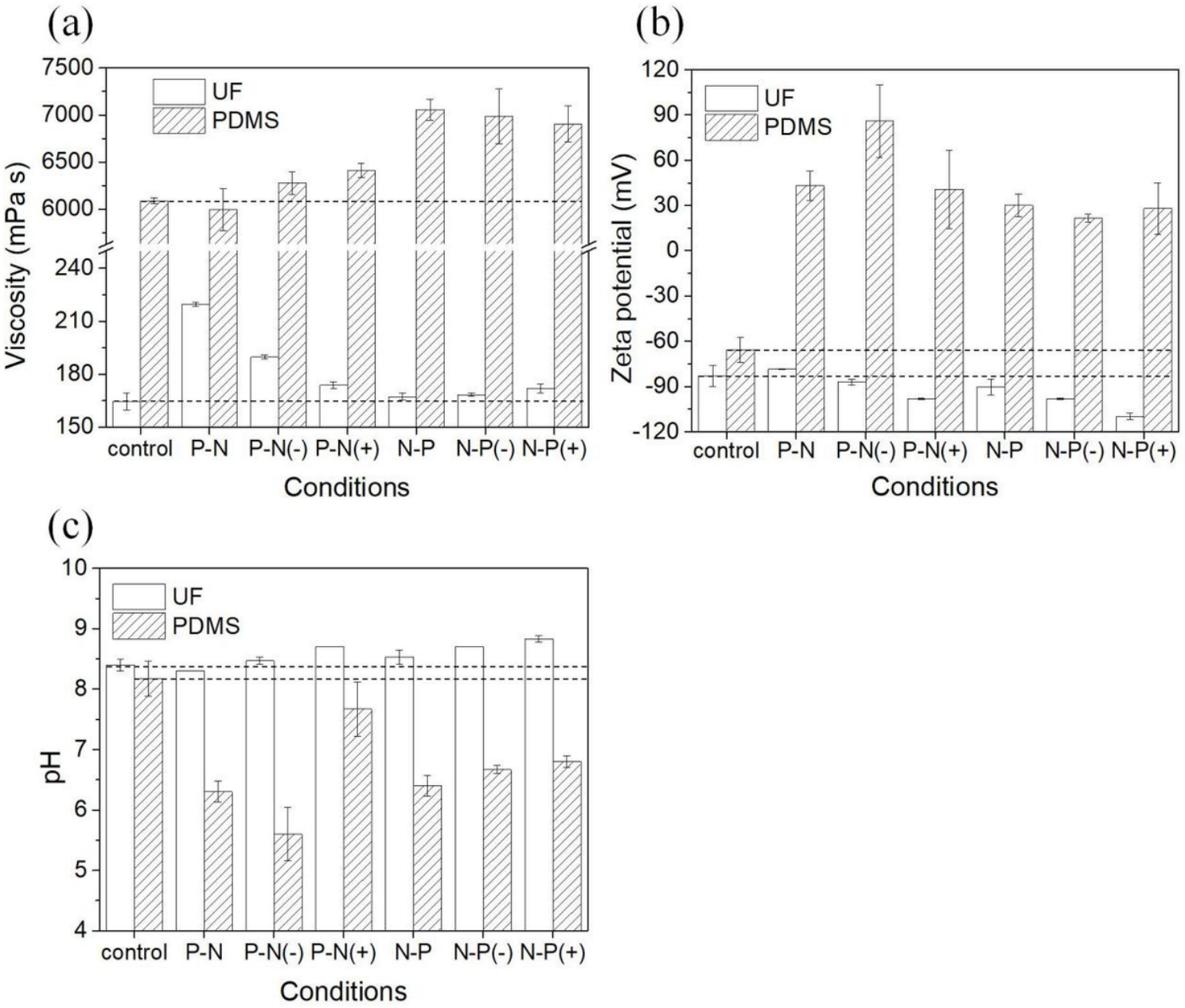

Figure 3

The characteristics of UF and PDMS coatings treated after the HVEF treatment and compared with the control including (a) viscosity, (b) zeta potential and (c) pH.

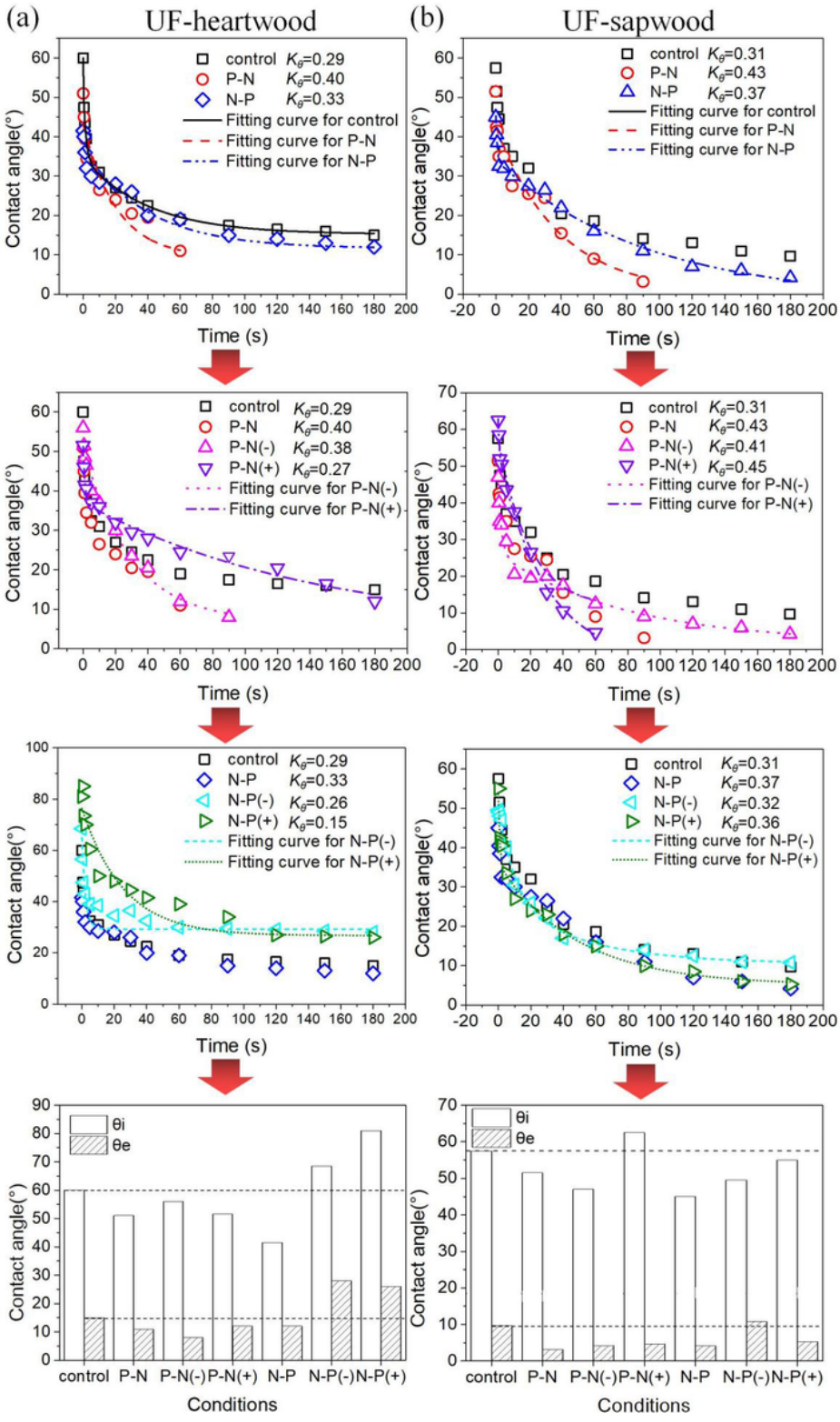

Figure 4

The contact angle of UF on Chinese fir (a) heartwood and (b) sapwood depending on the wetting duration under the HVEF treatment compared with the control.

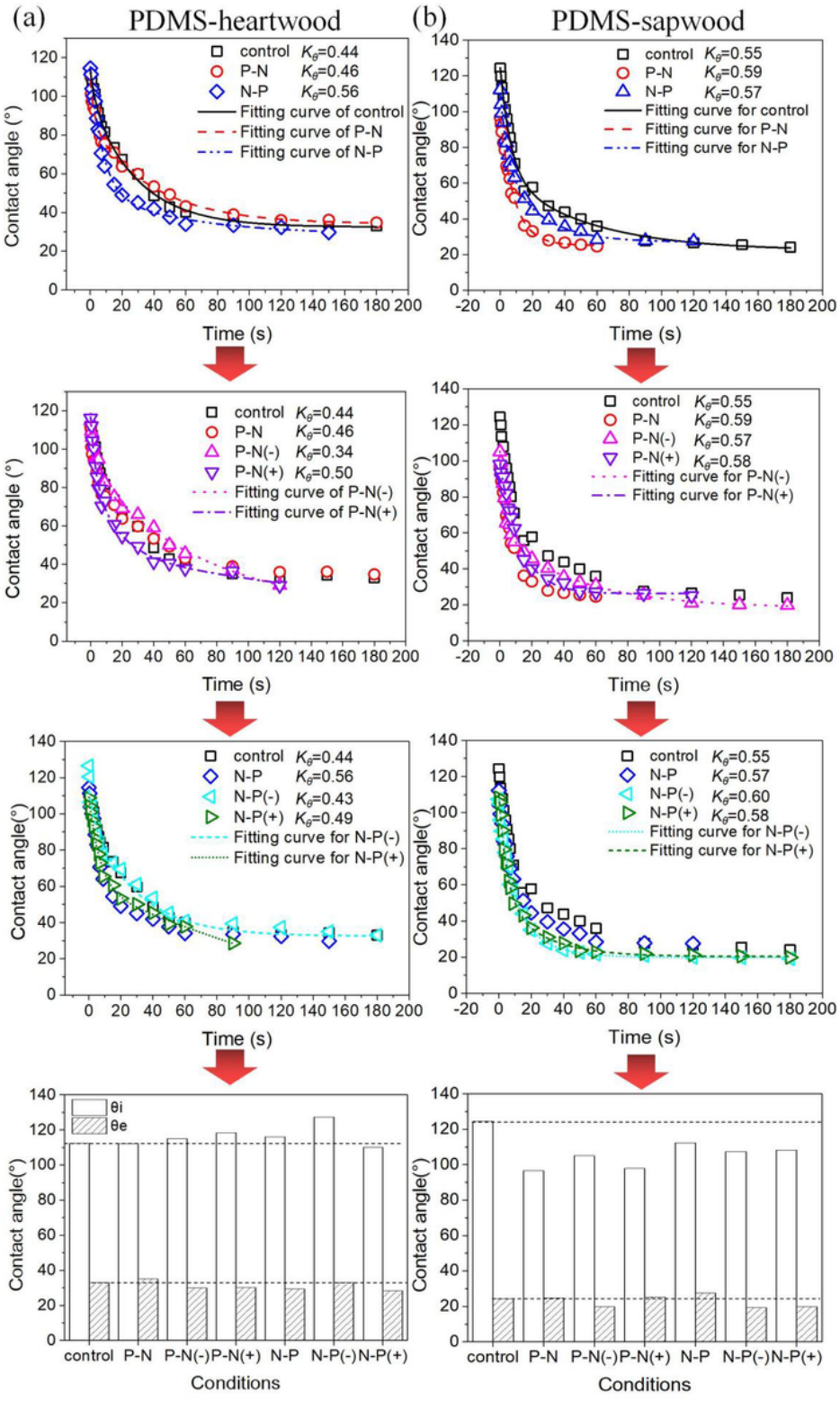

Figure 5

The contact angle of PDMS on Chinese fir (a) heartwood and (b) sapwood depending on the wetting duration under the HVEF treatment compared with the control.

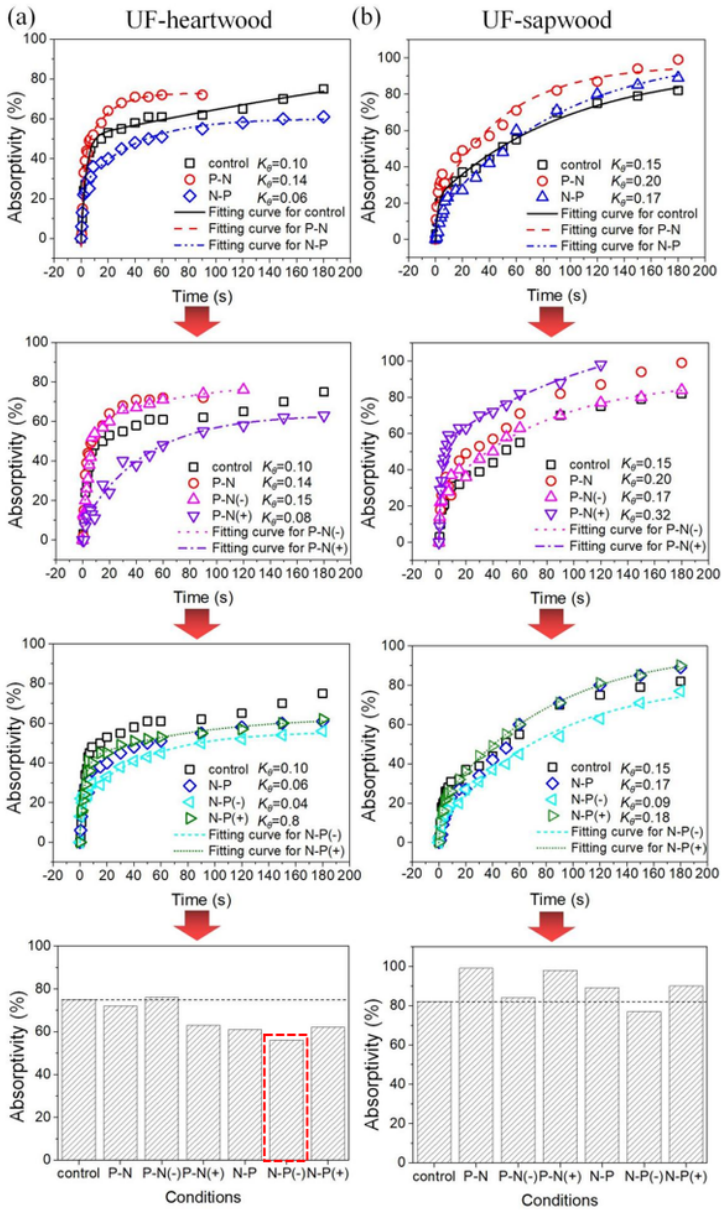

Figure 6

The absorptivity of UF on Chinese fir (a) heartwood and (b) sapwood depending on the wetting duration under the HVEF treatment compared with the control.

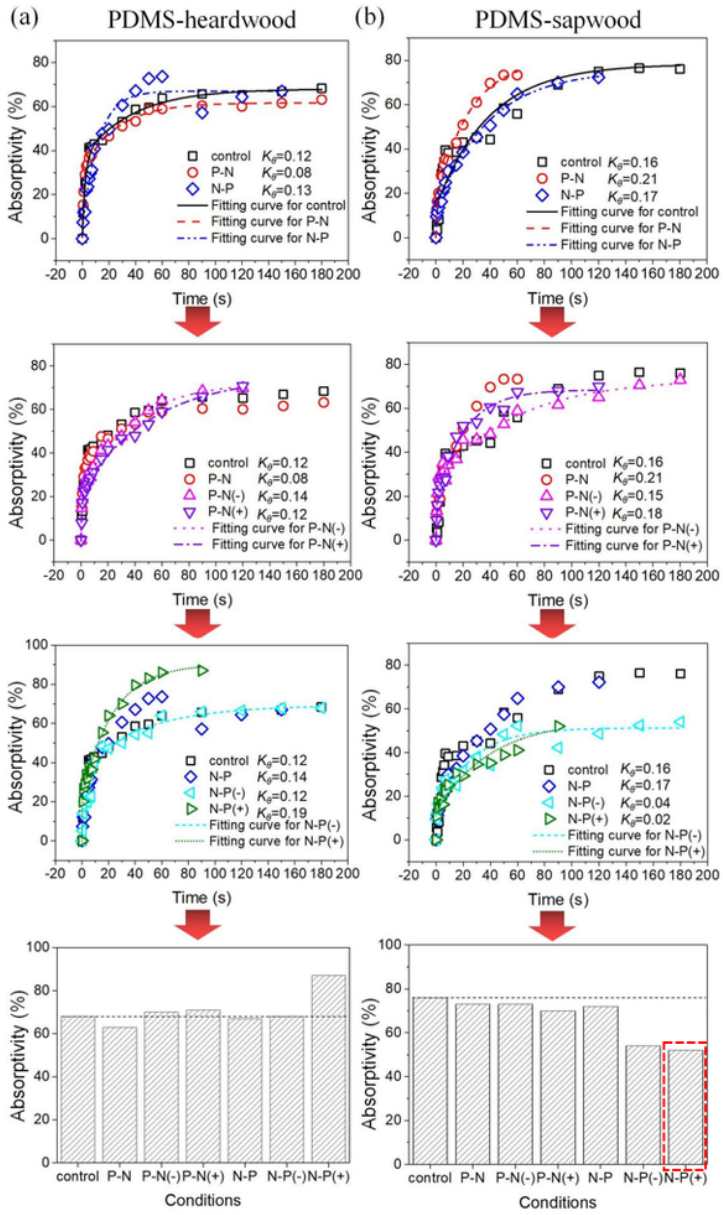

Figure 7

The absorptivity of PDMS on Chinese fir (a) heartwood and (b) sapwood depending on the wetting duration under the HVEF treatment compared with the control.

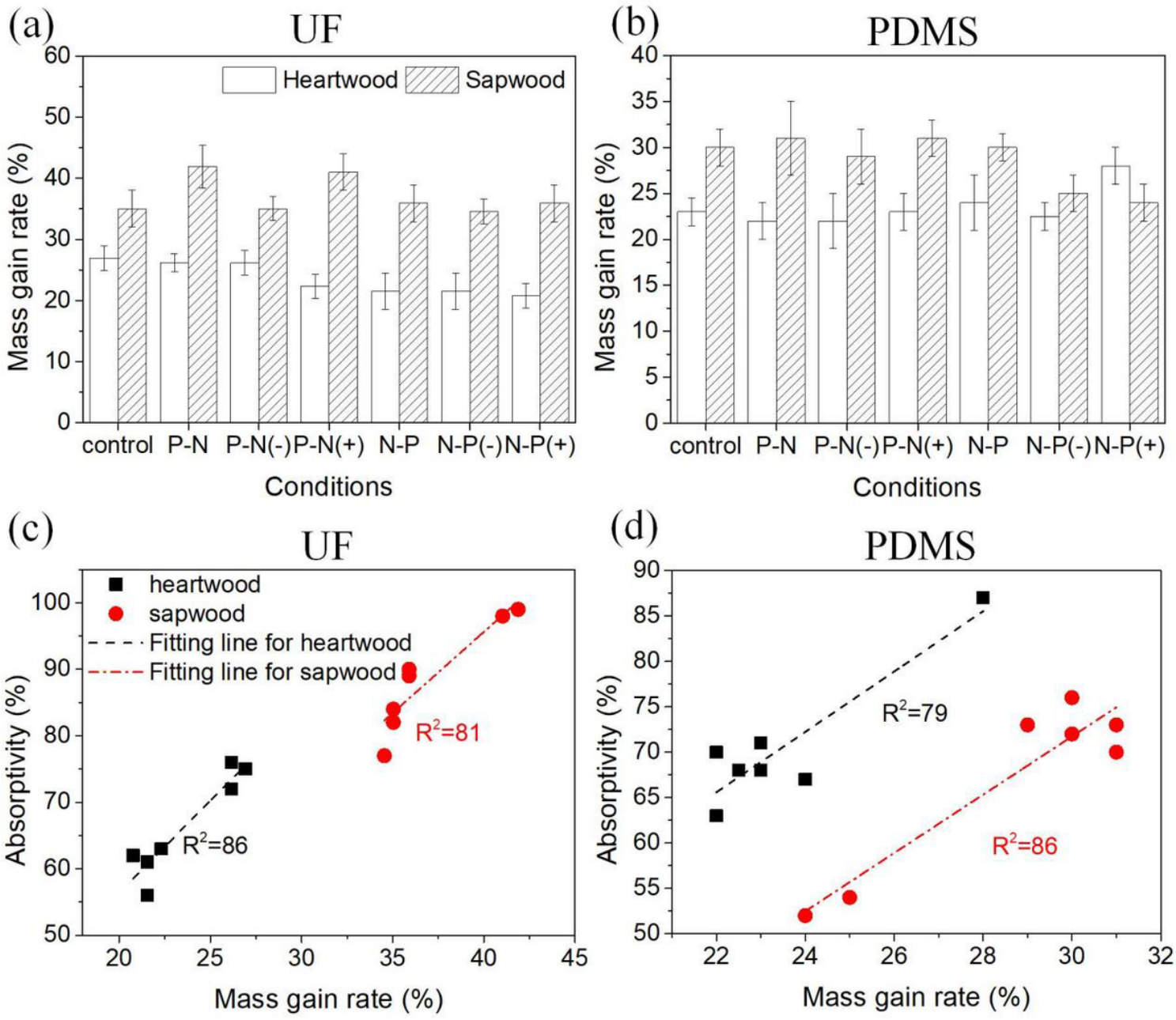

Figure 8

The mass gain rate of (a) UF- and (b) PDMS-coated wood samples, respectively under the HVEF treatment with the comparison of the control and its relationship with the absorptivity of (c) UF and (d) PDMS on Chinese fir, respectively.

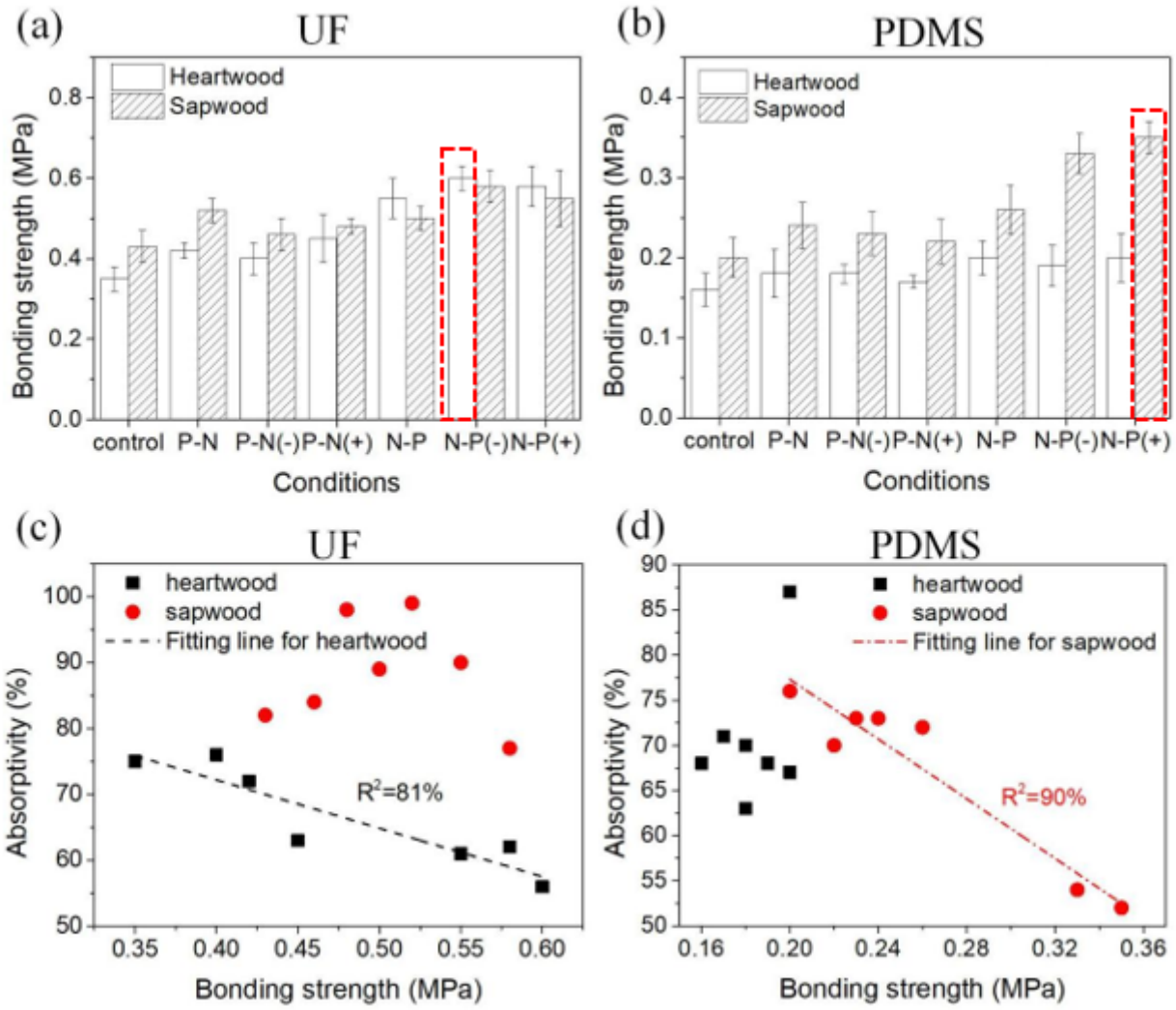

Figure 9

The bonding strength of (a) UF and (b) PDMS coating layer with Chinese fir, respectively under the HVEF treatment with the comparison of the control and its relationship with the absorptivity of (c) UF and (d) PDMS on Chinese fir, respectively.

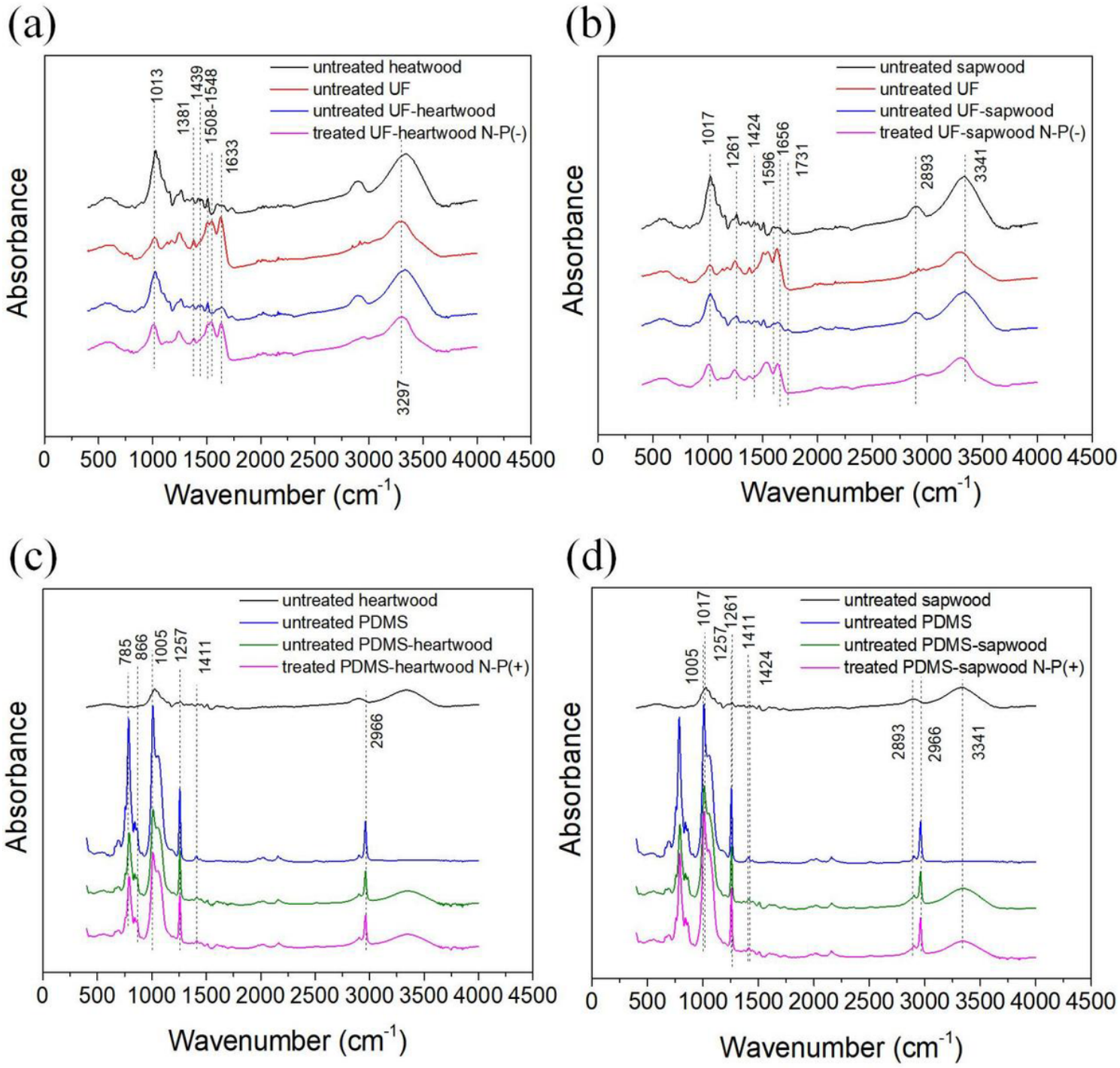

Figure 10

The FTIR spectra for (a) UF-coated heartwood, (b) UF-coated sapwood samples under N-P(-) condition and the spectra for (c) PDMS-coated heartwood, (d) PDMS-coated sapwood samples under N-P(+) condition compared with the untreated samples.